Current Biology, Vol. 13, 2148–2158, December 16, 2003, ©2003 Elsevier Science Ltd. All rights reserved. DOI 10.1016/j.cub.2003.11.027

Structure and Function of the Conserved Core of Histone Deposition Protein Asf1

Sally M. Daganzo,[1,2,5] Jan P. Erzberger,[2] Wendy M. Lam,[1,2] Emmanuel Skordalakes,[2] Rugang Zhang,[3] Alexa A. Franco,[1,2] Steven J. Brill,[4] Peter D. Adams,[3] James M. Berger,[2] and Paul D. Kaufman[1,2,*]

[1]Lawrence Berkeley National Laboratory and
[2]Department of Molecular and Cell Biology
University of California, Berkeley
Berkeley, California 94720
[3]Fox Chase Cancer Center
Philadelphia, Pennsylvania 19111
[4]Rutgers University
Department of Molecular Biology and Biochemistry
CABM–679 Hoes Lane
Piscataway, New Jersey 08854

Summary

Background: Asf1 is a ubiquitous eukaryotic histone binding and deposition protein that mediates nucleosome formation in vitro and is required for genome stability in vivo. Studies in a variety of organisms have defined Asf1's role as a histone chaperone during DNA replication through specific interactions with histones H3/H4 and the histone deposition factor CAF-I. In addition to its role in replication, conserved interactions with proteins involved in chromatin silencing, transcription, chromatin remodeling, and DNA repair have also established Asf1 as an important component of a number of chromatin assembly and modulation complexes.

Results: We demonstrate that the highly conserved N-terminal domain of *S. cerevisiae* Asf1 (Asf1N) is the core region that mediates all tested functions of the full-length protein. The crystal structure of this core domain, determined to 1.5 Å resolution, reveals a compact immunoglobulin-like β sandwich fold topped by three helical linkers. The surface of Asf1 displays a conserved hydrophobic groove flanked on one side by an area of strong electronegative surface potential. These regions represent potential binding sites for histones and other interacting proteins. The structural model also allowed us to interpret mutagenesis studies of the human Asf1a/HIRA interaction and to functionally define the region of Asf1 responsible for Hir1-dependent telomeric silencing in budding yeast.

Conclusions: The evolutionarily conserved, N-terminal 155 amino acids of histone deposition protein Asf1 are functional in vitro and in vivo. This core region of Asf1 adopts a compact immunoglobulin-fold structure with distinct surface characteristics, including a Hir protein binding region required for gene silencing.

*Correspondence: pdkaufman@lbl.gov
[5]Present address: School of Medicine, University of California, San Francisco, San Francisco, CA 94143.

Introduction

The fundamental structural units of eukaryotic chromosomes are nucleosomes, particles composed of DNA wrapped around octamers of histone proteins. During replication, new nucleosomes are assembled through the directed deposition of histones onto newly replicated DNA [1, 2]. Nucleosome assembly is a two-step process initiated by the deposition of a histone $(H3{\cdot}H4)_2$ tetramer on DNA, followed by the addition of two histone (H2A·H2B) dimers. This ordered mechanism of histone addition is critical for proper nucleosome formation in vivo and is regulated by nucleosome assembly factors that bind histones and mediate their interactions with DNA (reviewed in [3, 4]).

One nucleosome assembly protein, Asf1, was originally discovered through genetic studies in budding yeast as a factor that antagonized chromatin-mediated gene silencing when overexpressed [5, 6]. *S. cerevisiae* cells lacking Asf1 display increased frequencies of spontaneous genome rearrangements [7], nonviability in the presence of double-strand DNA breaks [8], and a dependence on genes involved in transcriptional elongation for viability [9]. The fission yeast homolog of Asf1, the CIA1 protein, is essential for viability [10].

Several biochemical studies have directly linked Asf1 to chromatin assembly after DNA replication. For example, *Drosophila* Asf1 binds newly synthesized histone H3/H4 tetramers to form a complex that stimulates the histone deposition activity of chromatin assembly factor-I (CAF-I) through a direct interaction with its Cac2/p60 subunit [11–14]. Asf1 also interacts directly with chromatin assembly factors of the Hir1/HIRA family to support the formation of silent chromatin and to regulate histone gene transcription and S phase progression [15–20]. Asf1 may also mediate chromatin assembly following DNA damage through a direct interaction with the S phase damage checkpoint kinase Rad53 [21, 22].

In addition to its function in nucleosome assembly during DNA replication and DNA repair, Asf1 has conserved roles in other aspects of DNA metabolism. Asf1 has been shown to interact with the histone acetyltransferase complex SAS-I [15, 23, 24], the chromatin remodeling enzyme Brahma [25], and the basal transcription factor TFIID component $TAF_{II}250$/CCG1 [26, 27]. The complex interplay of Asf1 with its various partner proteins is illustrated by the fact that Asf1 binding to Rad53 and histones H3/H4 is mutually exclusive [21, 22]. Similarly, Asf1 occludes bound histones from modification by the SAS-I histone acetyltransferase complex [28], suggesting that these proteins may compete for a small number of binding surfaces. To date, there is little understanding of the molecular details that enable Asf1 to mediate such a diverse array of functions.

As a first step toward understanding Asf1 function, we report here biochemical and structural studies of the evolutionarily conserved N-terminal domain of the Asf1 protein. Our results show that this core domain adopts a β sandwich fold that is sufficient to recapitulate various

aspects of full-length Asf1 function. Structural features and residue conservation reveal regions of the protein that are candidate protein interaction surfaces and have allowed us to define a Hir1 interaction surface on Asf1 responsible for in vivo telomere silencing.

Results and Discussion

Asf1 Amino Acids 1–155 (Asf1N) Are Functional In Vivo and In Vitro

Saccharomyces cerevisiae Asf1 comprises 279 amino acids distributed into two distinct regions. The first 155 amino acids are highly conserved among eukaryotic species (65%–90% identity) and have predicted secondary structure elements. The C-terminal region (<15% identity) is poorly conserved and is predicted to consist largely of disordered coils. The C-terminal region does contain long poly-acidic tracts in fungi, but this feature is not conserved in other eukaryotes. For example, in *Leishmania major* Asf1, the C-terminal region is lacking altogether. These observations, together with a previous study showing that a fragment of the *S. cerevisiae ASF1* gene comprising amino acids 1–169 is sufficient to restore viability to fission yeast mutants lacking the homologous *cia1* gene [10], suggested that a minimal core region comprising the conserved N-terminal 155 amino acids of budding yeast Asf1 might be biologically functional. We will refer to this N-terminal region as the Asf1N protein.

S. cerevisiae cells lacking the *ASF1* gene are sensitive to the DNA damaging agent methyl methanesulfonate (MMS) and to the ribonucleotide reductase inhibitor hydroxyurea (HU) [11]. To determine whether Asf1N could complement the DNA damage sensitivity of *asf1*Δ strains, we introduced plasmids expressing Asf1 or Asf1N and exposed the cells to MMS or HU. Our results demonstrate that the N-terminal domain of Asf1 is as proficient as the wild-type protein to confer resistance to DNA damaging agents in vivo (Figure 1A).

Asf1 stimulates the activity of CAF-I in vitro and contributes to chromatin-mediated silencing in vivo in a manner that overlaps CAF-I [11–14, 16]. Yeast cells lacking both the *ASF1* gene and any of the three CAF-I subunits encoded by the *CAC1*, *CAC2*, and *CAC3* genes display slow growth and possess poor chromatin-mediated gene silencing [11, 16]. To define the region of Asf1 responsible for mediating these effects, we compared growth rates and telomere-proximal gene silencing in *cac1*Δ *asf1*Δ double mutants expressing either full-length Asf1 or the truncated Asf1N protein (Figure 1B). In our growth assays, plasmids encoding either Asf1 or Asf1N restored wild-type growth rates to *cac1*Δ *asf1*Δ cells (Figure 1B, left). To assess gene silencing, we used a *URA3* reporter gene inserted adjacent to telomere VIIL and measured growth on media containing FOA, a metabolic toxin that positively selects for the ability to silence the *URA3* gene [29]. As previously observed, *cac1*Δ mutants display a partial loss of telomeric silencing, and *cac1*Δ *asf1*Δ double mutants display a severe loss of silencing [11, 30]. In the *cac1*Δ *asf1*Δ double mutant cells, however, plasmids encoding either Asf1 or Asf1N restored telomeric silencing to levels observed in *cac1*Δ cells (Figure 1B, right). Taken together, these data provide strong support that Asf1 and Asf1N are equally competent to mediate the assembly of silenced chromatin in vivo.

In vitro, Asf1 is a histone H3/H4 binding and deposition protein [10, 11, 16, 31]. To determine whether Asf1N retains this function in vitro, we performed coprecipitation experiments with purified histones H3/H4 and recombinant, epitope-tagged Asf1 and Asf1N. Both Asf1 and Asf1N retained similar amounts of histones after extensive washing with buffer containing 250 mM NaCl, demonstrating that Asf1N is a functional histone binding protein (Figure 1C). Histone binding to Asf1N was more easily disrupted by high salt concentrations, however, suggesting that the acidic C terminus interacts with the H3/H4 tetramer, perhaps through electrostatic contacts with the basic histone proteins.

Another binding partner of Asf1 is the Rad53 protein [21, 22], a cell cycle checkpoint kinase that interacts with Asf1 through one of its forkhead-associated (FHA) domains [32]. In coprecipitation experiments, Asf1N retained similar amounts of Rad53 compared to Asf1 (Figure 1D), demonstrating that Asf1N is a functional Rad53 binding protein. These data are consistent with the ability of Asf1N to provide protection from DNA damaging agents (Figure 1A). In addition, the interaction between Rad53 and Asf1N depended on enzymatic dephosphorylation of the Rad53 protein preparation (data not shown). This finding agrees with previous data demonstrating that the Asf1-Rad53 interaction is regulated by phosphorylation of Rad53 [21, 22, 32].

In vitro, Asf1 stimulates histone deposition by substoichiometric amounts of CAF-I [11, 13]. To test whether Asf1N could also stimulate histone deposition by CAF-I, we turned to in vitro DNA replication reactions. In these assays, nucleosome formation is detected by the supercoiling of circular, replicated DNA templates that have been labeled by incorporation of a radioactive deoxynucleotide. We observed that both full-length Asf1 and Asf1N were able to stimulate nucleosome formation by a substoichiometric amount of CAF-I (Figure 1E) and that the specific activity of Asf1N in this assay was as high, if not higher, than that of full-length Asf1. As observed previously for Asf1, the amount of Asf1N required to stimulate CAF-I was unable to promote efficient histone deposition alone (lanes 6–8 and 12–14; [11, 13]), reflecting the functional synergy between these histone deposition factors. We conclude that Asf1N is functional for histone binding and stimulation of histone deposition by CAF-I in vitro.

Structure of Asf1N

To explore the molecular basis of the many functional interactions of Asf1N, we overexpressed the recombinant protein in *E. coli* and purified it to homogeneity for structural studies (see Experimental Procedures). Contrary to full-length Asf1, the purified truncated protein did not aggregate in solution (data not shown), and crystals of Asf1N were readily obtained by the hanging-drop vapor-diffusion method from a variety of conditions using PEG3350 as the precipitant. The crystals belong to space group C2 and contain one Asf1N monomer per asymmetric unit.

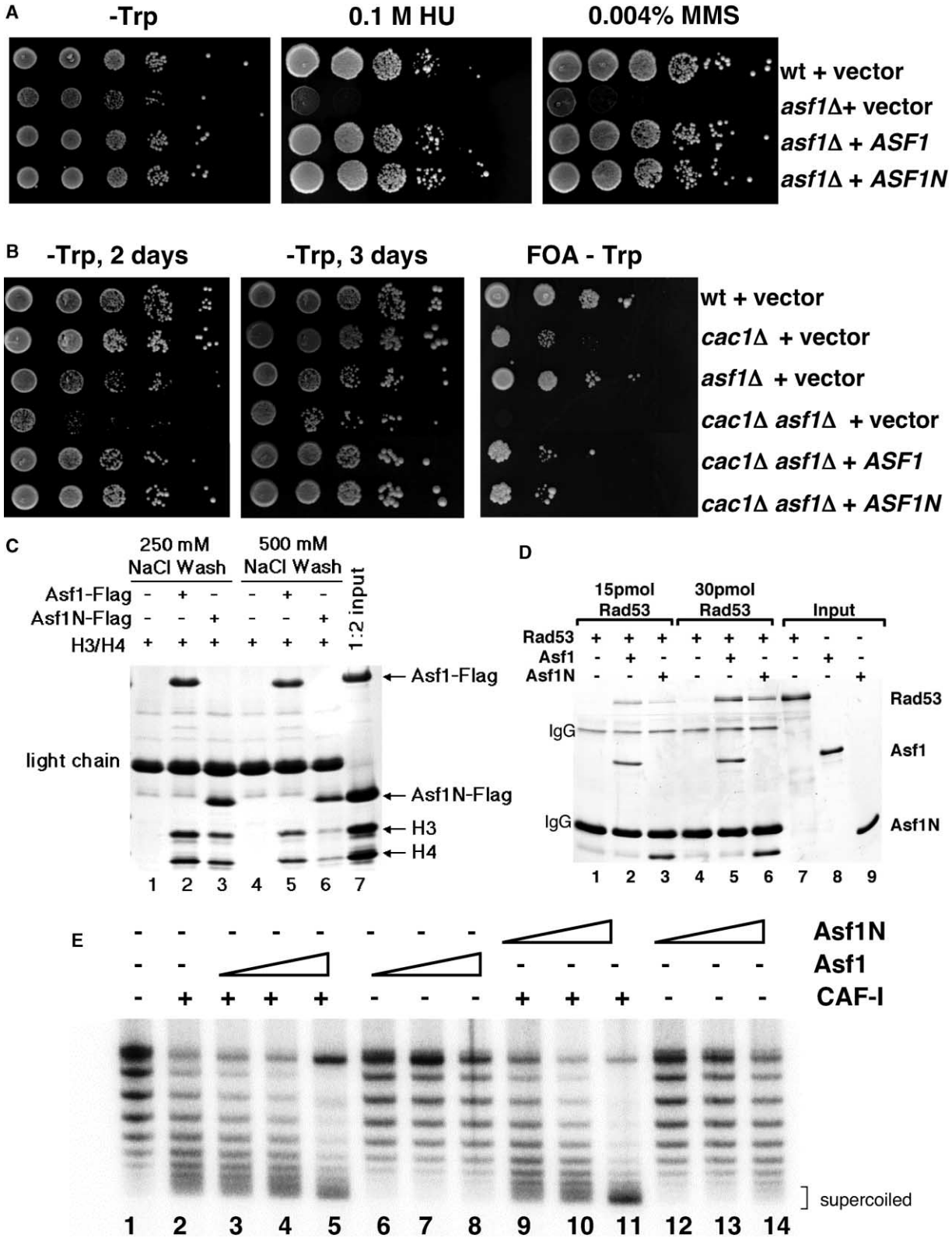

Figure 1. Yeast Asf1N Protein Is Functional In Vitro and In Vivo

(A) Asf1N confers DNA damage resistance in vivo. Yeast strains of the indicated genotypes were transformed with low-copy plasmids expressing full-length Asf1, Asf1N, or an empty vector as indicated. Strains were grown to logarithmic phase, serially diluted, and spotted onto synthetic complete media lacking tryptophan (-Trp) to score total plasmid-containing cells or onto media containing 0.004% methyl methanesulfonate (MMS) or 0.1 M hydroxyurea (HU).

We determined the structure of Asf1N to a resolution of 1.5Å using multiwavelength anomalous dispersion methods on crystals grown in high concentrations of bromide ions (Figure 2A) (Table 1). The first 155 residues of Asf1 fold into an elongated (20Å × 25Å × 55Å) β sandwich domain topped by α helices. The fold adopted by Asf1N belongs to the "switched" immunoglobulin class of proteins (Figure 2B) [33], a broad group of structures that in addition to immunoglobulins includes type III fibronectins and cadherins [34]. A search of the structural database [33] shows that Asf1N most closely superposes human type III fibronectin (2fnb: RMSD 2.7Å) [35] and the Rho guanine nucleotide dissociation inhibitor RhoGDI (1rho: RMSD 2.9Å) [36].

An analysis of surface electrostatic potential, curvature, and amino acid conservation highlights three regions of Asf1N that may be important for its various functions (Figures 2C and 3). The first and most striking of these is a concave groove on the front of the molecule that is principally hydrophobic in character (Figure 3A). The concavity of the groove is established by the curvature of the larger of the two β sheets, by the hairpin turn between strands β7 and β8, and by the β4/β5 connector loop (Figure 2B). The groove is decorated with a number of conserved, solvent-exposed hydrophobic residues, including V45, V92, L96, and Y112, and represents a potential protein-protein interaction surface.

Flanking the groove lies a second region of interest, which is defined by a strongly electronegative surface potential arising from a cluster of acidic residues on β4 and β5 (D37, E39, D58, and D77). Many of these show a high degree of conservation (Figure 3B). Given the proximity of this region to the hydrophobic groove and because electronegative surfaces have previously been implicated as histone binding determinants [37], the acidic region of Asf1 represents a likely histone interaction site. However, some residues in this region also appear to be essential for stability of Asf1, because a double E39A, K41A mutation resulted in nearly undetectable levels of Asf1 by immunoblotting of cell extracts. Additionally, the Asf1$^{E39A, K41A}$ protein was nonfunctional for in vivo HU sensitivity and silencing assays (data not shown).

The third region of interest lies on the other side of the hydrophobic groove. This area, which lies near the base of Asf1N between strands β1 and β10, contains a deep pocket near the N and C termini that is lined with hydrophobic residues (Figure 3B). The pocket is connected to a narrow channel that runs along the entire edge of the Asf1N molecule (Figure 3). While narrower than the groove, the cleft appears sufficiently wide to accommodate an additional β strand from an interacting protein to pair with β1. Indeed, it is worth noting that in other switched Ig-fold proteins, a fourth strand is found at this position [34]. The top of the molecule is decorated with two small α-helical elements (α1 and α2) and a short 3-10 helix (α3) that appear to be present in all organisms and to be moderately well conserved (Figure 2C), providing another potential interaction region.

The Hir1 Binding Site on Asf1

In budding yeast, Asf1 and the Hir proteins physically interact and function together to support the formation of silent chromatin and regulate histone gene transcription [15, 16]. While budding yeast has a single Asf1 protein, mammals retain two closely related proteins termed Asf1a and Asf1b along with a Hir1/Hir2 homolog known as HIRA. We hypothesized that the Asf1-Hir protein interaction might be conserved in evolution and that we could use our structural data to define regions of Asf1 important for this interaction.

To test these ideas, we first investigated the human Asf1a and HIRA proteins because we had observed interaction between these proteins in two-hybrid experiments (data not shown); the interaction of Asf1b and HIRA is under investigation. We confirmed a direct, stable interaction between Asf1a and HA-epitope-tagged HIRA in coprecipitation experiments using HA-epitope-tagged HIRA (Figure 4A). Alanine-substituted mutant human Asf1a proteins were then used to define potential binding sites for HIRA on Asf1a. Mutation of either of two sets of contiguous amino acids in human Asf1a, amino acids 36–37(ED to AA) and 62–64(VGP to AAA), completely abolished Asf1a-HIRA interactions. In contrast, alanine substitutions in at least four different regions of Asf1a have no effect on HIRA binding including: (1) Asp13, which lies in the region between β strands 1 and 2, (2) Glu49 and Glu51, which reside in the β4/β5 connector turn, (3) Asp77, which is located at the end of strand β6, and (4) Glu121 and Glu124 of helix α2.

To determine whether the human Asf1a mutations might define a single HIRA binding site, we mapped their position on the yeast Asf1N structure. Indeed, both sets of mutations lie proximally to each other on the surface of Asf1 (Figure 3B). In contrast, several other mutations that did not affect HIRA binding were distributed elsewhere on the tertiary structure. H36 and D37 are located on a loop immediately preceding β4, while

(B) Asf1N promotes chromatin-mediated gene silencing at telomeres. Cells of the indicated genotypes containing an *URA3-VIIL* telomeric reporter gene were transformed with plasmids expressing full-length Asf1, Asf1N, or an empty vector as indicated. Strains were grown to logarithmic phase, serially diluted, and plated as indicated onto -Trp media to assess total cell number or onto FOA-Trp to measure silencing.
(C) Asf1N binds to histones H3/H4. Recombinant FLAG-epitope-tagged Asf1 or Asf1N were incubated with histones H3/H4, immunoprecipitated with anti-FLAG antibodies coupled to a solid resin, and the precipitates were washed as indicated. Retained proteins were visualized by Coomassie staining of a 17% SDS-PAGE gel.
(D) Asf1N binds to Rad53. 15 pmol (lanes 1–3) or 30 pmol (lanes 4–6) of recombinant, dephosphorylated Rad53 was incubated with no protein (lanes 1 and 4) or 15 pmol FLAG-epitope-tagged Asf1 (lanes 2 and 5) or Asf1N (lanes 3 and 6) and immunoprecipitated with anti-FLAG antibodies. Input lanes contain 15 pmol of each protein (lanes 7–9). Proteins were visualized by Coomassie staining of a 15% SDS-PAGE gel.
(E) Asf1N stimulates the replication-coupled histone deposition activity of CAF-I. Where indicated, a substoichiometric amount of recombinant yeast CAF-I (12 ng, [13]) was added. Preformed Asf1·$(H3{\cdot}H4)_2$ or Asf1N·$(H3{\cdot}H4)_2$ complexes were titrated into the reactions at 0.44, 0.88, or 1.75 pmol of histone tetramer in lanes 3–5, 6–8, 9–11, and 12–14, respectively. Stimulation of histone deposition is indicated by the increased proportion of supercoiled DNA, as observed in lanes 5 and 11.

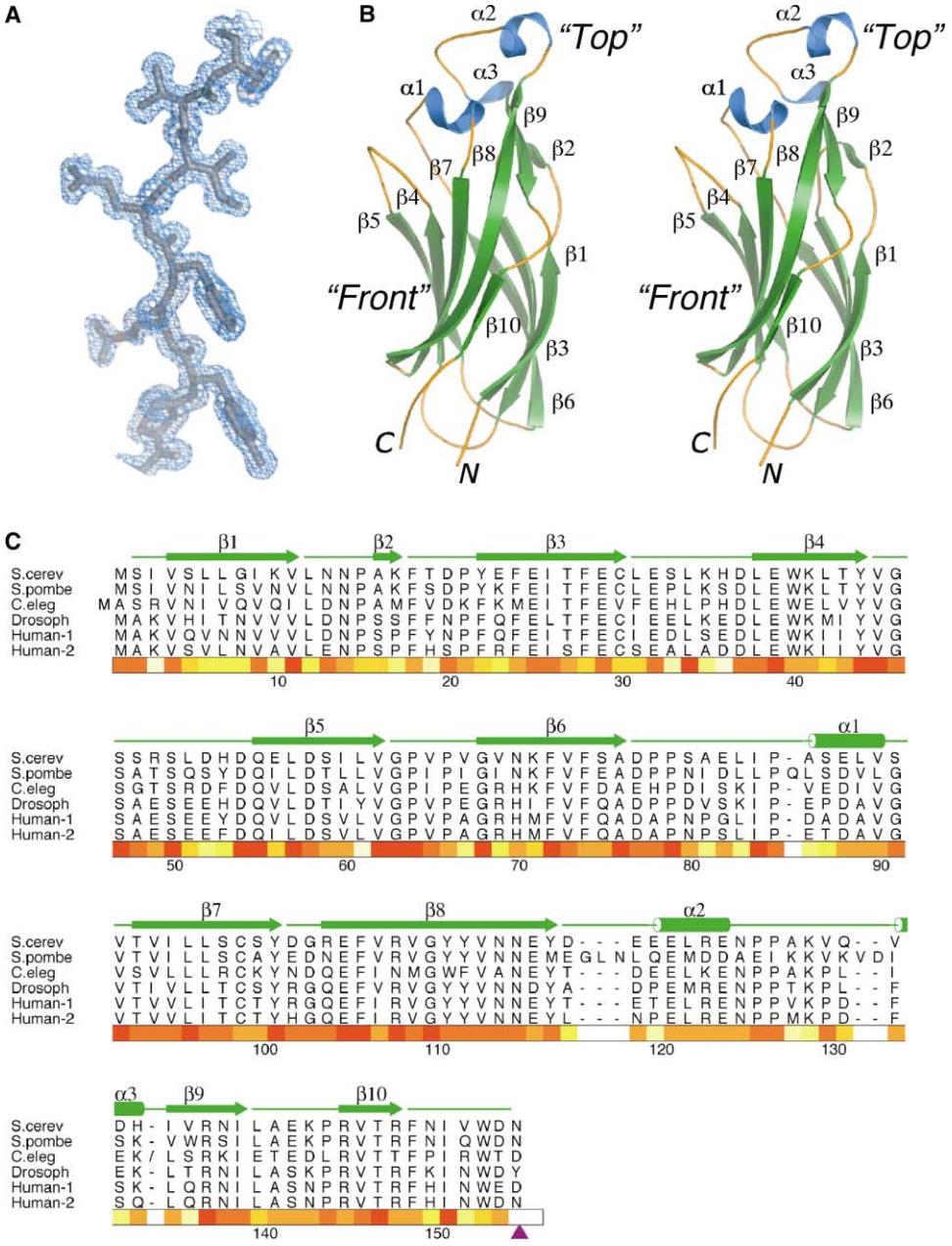

Figure 2. Backbone Structure and Amino Acid Conservation of Asf1N

(A) A portion of the 1.5 Å resolution experimental electron density map contoured at 1σ from the region around strand β3.

(B) Stereo view of a ribbon diagram of Asf1N illustrating the secondary structure elements. This view faces the hydrophobic cleft between strands β1 and β10 (see Figure 3).

(C) Comparison of Asf1 protein sequences and structure. Secondary structure elements are labeled over sequences and match those indicated in (B). The degree of evolutionary conservation as determined using clustalX [56] is shown as a gradient of red, orange, yellow, and white boxes, with red being most highly conserved and white being nonconserved. The purple triangle at the end of the sequence marks the natural termination point of the *Leishmania* Asf1 protein.

(A) and (B) were rendered using PYMOL [57]. (C) was generated using ALSCRIPT [58]. Human-1 refers to the Asf1a protein (accession number CAB43363) and Human-2 refers to the Asf1b protein (accession number NP_060624).

conserved residues V62, G63, and P64 define the end of strand β5. These amino acids all lie adjacent to the hydrophobic groove, and D37 is a component of the acidic region (Figure 3B). A comparison of Asf1 proteins shows that residues 62–64 (VGP) are nearly completely identical throughout all eukaryotes (Figure 2C). P64 is one of two cis-prolines present in Asf1N, the other being P15 at the turn between the β1 and β2 strands. Along with G63, P64 is responsible for a sharp turn in the loop immediately after β5. This arrangement anchors the loop connecting β5 and β6 into a rigid, structured element. The loss of this element would compromise the struc-

Table 1. Structure Determination Statistics

Data Collection			
	Remote	Peak	
Radiation Å	0.956	0.920	
Resolution Å	50–1.5	50–1.6	
Completeness % (last shell)	94.0 (82.4)	91.6 (61.9)	
Overall I/σ (last shell)	13.45 (2.6)	11.3 (1.7)	
[a]R_{sym} % (last shell)	5.3 (23.9)	6.7 (28.8)	
Phasing			
Atom	Br		
Number of sites	9		
Mean figure of merit	0.39		
Structure Refinement			
Resolution range (Å)	30-1.5	Overall reflections (last shell)	19972 (1343)
Number of nonhydrogen atoms	1402	Test reflections (last shell)	1082 (85)
Number of protein atoms	1235	R_{work}/R_{free}[b] (%)	19.77/24.65
Number of ligand atoms	9	$Rmsd_{bonds/angles}$	0.009/1.094
Number of water atoms	158	Ramachandran % (no res.)	
		Most favored	92.7 (127)
		Allowed	6.6 (9)
		Gen. allowed	0.7 (1)

[a] $R_{sym} = \Sigma\Sigma_j|I_j - <I>|/\Sigma I_j$, where I_j is the intensity measurement for reflection j and $<I>$ is the mean intensity for multiply recorded reflections.
[b] $R_{work, free} = \Sigma||F_{obs}| - |F_{calc}||/\Sigma|F_{obs}|$, where the working and free R factors are calculated using the working and free reflection sets, respectively. The test reflections (5.2% of the total) were held aside throughout refinement.

tural integrity of this region. The VPG to AAA change is therefore likely to change the local backbone fold as well as the surface characteristics. On the neighboring loop immediately adjacent to the VPG sequence lies H36/D37. Of these two residues, only D37 is highly conserved, suggesting that D37 is more likely to play a key role in mediating Hir1 binding than H36. Further characterization should determine whether Hir1 binding determinants extend into either the acidic region or the conserved groove of Asf1.

To confirm these findings and examine their importance in vivo, we recapitulated mutation of residues 36 and 37 in yeast Asf1. The Asf1$^{H36A, D37A}$ mutant restored the DNA damage resistance to cells lacking the chromosomal *ASF1* gene (Figure 4C), indicating that Asf1's role in DNA damage repair and normal cellular growth was not affected by this mutation. In contrast, in cells lacking both the *CAC1* and *ASF1* genes, the mutated Asf1$^{H36A, D37A}$ protein was unable to restore telomeric gene silencing (Figure 4D) even though normal levels of protein were present (Figure 4B). Because the *HIR1* gene cooperates with *ASF1* to contribute to silencing but does not have a role in DNA repair, these data are consistent with the idea that the contribution of the Asf1 and Hir1 proteins to silencing was specifically abolished by these mutations.

Comparison between Nucleoplasmin and Asf1

Although multiple histone binding and deposition proteins have been identified to date [3, 38, 39], structural information is only available for a few of these factors. Sequence analysis and secondary structure prediction have revealed that several deposition proteins, including two subunits of CAF-1 as well as HIRA-family proteins, contain WD repeats characteristic of β propeller structures [40, 41]. High-resolution crystallographic studies have provided a detailed view of two Nucleoplasmin (Np)-type proteins [37, 42, 43], a second class of histone binding and deposition factors that interact with H2A/H2B dimers and are abundant in *Xenopus* and *Drosophila* embryos [44, 45].

Nucleoplasmin (Np), like Asf1, adopts a β sandwich architecture. However, the Np fold is based on a jelly roll topology that is distinct from the Ig structure of Asf1N. Moreover, the functional unit of Np is a dimer of pentamers, whereas Asf1N does not oligomerize in solution. The different topologies and oligomerization states of Asf1N and Np-type proteins may reflect to the different biological roles of these proteins. For example, the multimeric arrangement of the Np protein core may promote the generation of high-avidity, stable Np-histone complexes to serve as embryonic histone storage elements, an important function of Np proteins [37]. One similarity does exist between Np and the fungal Asf1 homologs, namely the presence of extended, highly acidic C-terminal tails. While not essential for function in either protein, these regions nevertheless may act analogously to modulate electrostatic interactions between the deposition proteins, histones, and the target DNA. Interestingly, another yeast histone binding protein, Nap1, also possesses a nonessential acidic tail, and recent evidence indicates that these tails mediate the histone binding specificity of Nap1 [46].

While additional mutagenesis and cocrystallization experiments will be required to identify more fully the molecular determinants of histone recognition for Asf1 and other histone deposition factors, the structure of the Asf1 core region provides a starting point to define its role in histone deposition and nucleosome assembly.

Experimental Procedures

Yeast Strains and Plasmids

All yeast strains were in the W303 genetic background. The *asf1*Δ, *cac1*Δ, and *URA3-VIIL* alleles in this background have been de-

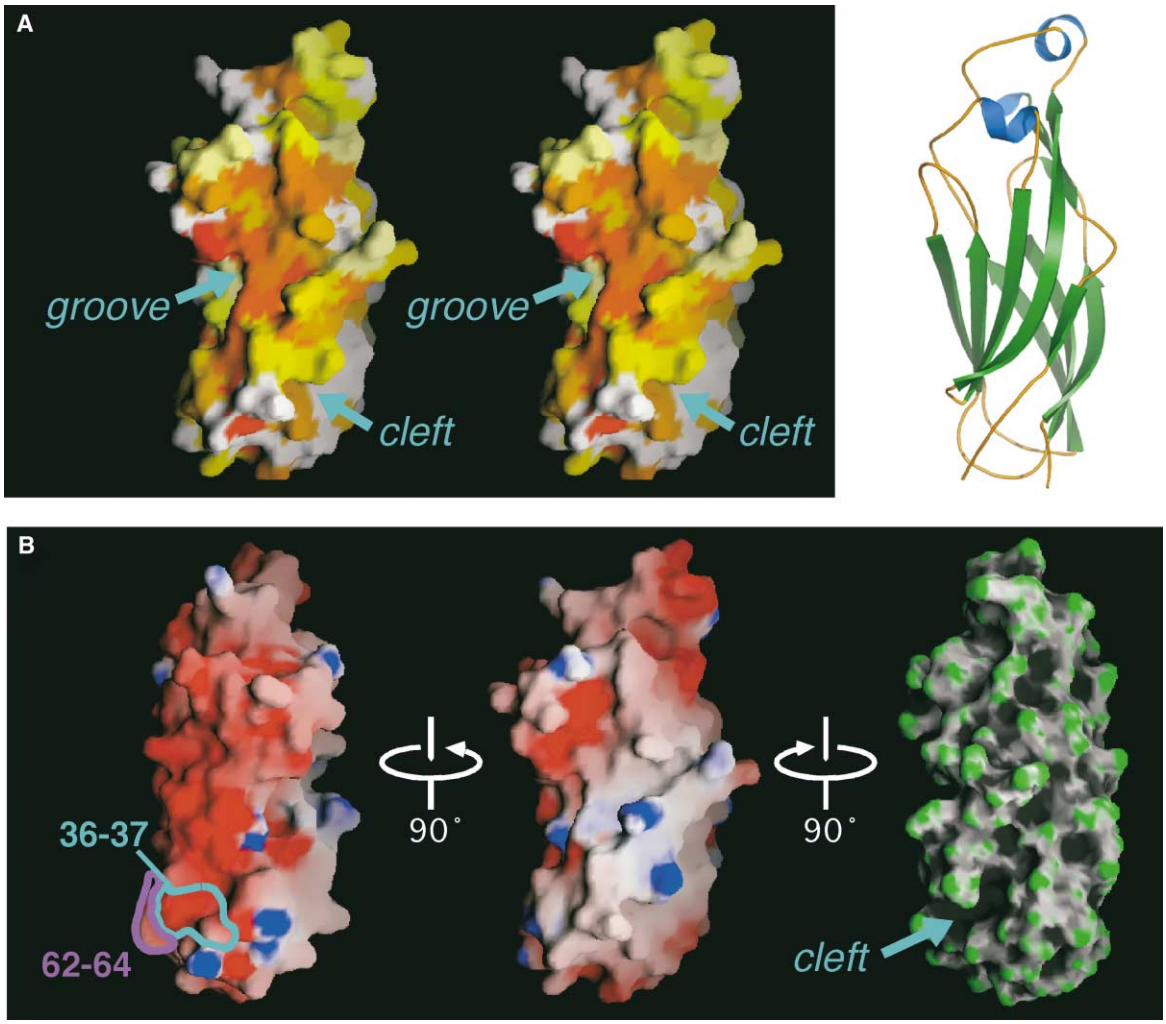

Figure 3. Surface Properties of Asf1N

(A) Conservation of residues on the front face. Left, stereo view of front face of Asf1N. The groove formed by the concave front sheet of β strands is labeled, as is the hydrophobic cleft between strands β1 and β10 that runs along the side of the protein. Coloration scheme is as in Figure 2C. Right, ribbon diagram of Asf1N secondary structure viewed from the same angle as the left panel.

(B) Electrostatic and curvature properties of Asf1N. The middle diagram shows the surface charge of the front view of the protein, viewed from the same angle as Figure 2A. Negative charge is shown in red, positive charge in blue. On the left, the diagram was turned 90° to the right to reveal the negatively charged surface formed largely by strands β4 and β5. On the right, the middle diagram was turned 90° to the left, and the concavity of the surface is highlighted with convex surfaces in green and concave surfaces in black. The deep hydrophobic cleft between strands β1 and β10 is labeled. Surface panels were generated with GRASP [59] and ribbon diagrams with PYMOL [57]. Amino acid conservation was mapped onto the protein surface in (A) using CONSURF [60]. Adjacent sets of residues implicated in Hir protein interaction are highlighted: residues 36–37 in cyan and 62–64 in violet.

scribed previously [16, 30]. Telomeric silencing assays using the *URA3-VIIL* reporter were also performed as previously described [16, 29]. For the damage sensitivity and silencing assays, cells were grown 2–3 days at 30°C before photographing, except for the FOA-Trp plates, which were grown for 6 days. For in vivo complementation experiments, the *ASF1* gene promoter was inserted into the *ARS/CEN, TRP1* vector pRS414 [47], and the full-length *ASF1* gene or the *ASF1N* fragment was inserted into this vector to allow for expression under control of the natural promoter.

Protein Expression and Purification

Hexa-histidine tagged Rad53 was overexpressed by insertion of the *RAD53* gene into pET28a (Novagen) to generate plasmid pHS4426. *E. coli* BL21(pLysS) cells containing pHS4426 were grown to exponential phase, and Rad53 expression was induced for 4 hr at 30°C by the addition of 1 mM IPTG. Frozen cell pellets from a 2 liter culture were resuspended in 25 mL Talon binding buffer (20 mM Tris-HCl [pH 8.0], 0.5 M NaCl, 0.01% NP40, 10 mM imidazole, 0.1 mM PMSF, 0.5 μg/mL leupeptin, 0.7 μg/mL pepstatin, 1 μg/mL aprotinin, and 1 μg/mL E64) and lysed by sonication. The extract was clarified by centrifugation and incubated with 1 mL of Talon immobilized metal resin (Clonetech) for 1 hr at 4°C. The resin was washed in batch twice with ten bed volumes of Talon binding buffer, and Rad53 was then eluted by addition of 10 mL Talon elution buffer (20 mM Tris-HCl [pH 8.0], 0.5 M NaCl, 0.01% NP40, 100 mM imidazole, and 0.1 mM PMSF). Rad53 was dephosphorylated by the addition of 4 units of Lambda Phosphatase (New England Biolabs) per μg of Rad53 in the buffer recommended by the manufacturer containing 0.2 mM $MnCl_2$. After incubating 40 min at 30°C, the protein was dialyzed into Talon binding buffer and purified away from the phosphatase by chromatography on Talon resin as above. Rad53 was stored in 25mM Tris-HCl [pH 7.5], 0.5 M NaCl, 1 mM EDTA, 0.01% NP40, 10% glycerol, 1 mM DTT, and 0.1mM PMSF.

C terminally FLAG-epitope-tagged Asf1N (Asf1N-FLAG) was ex-

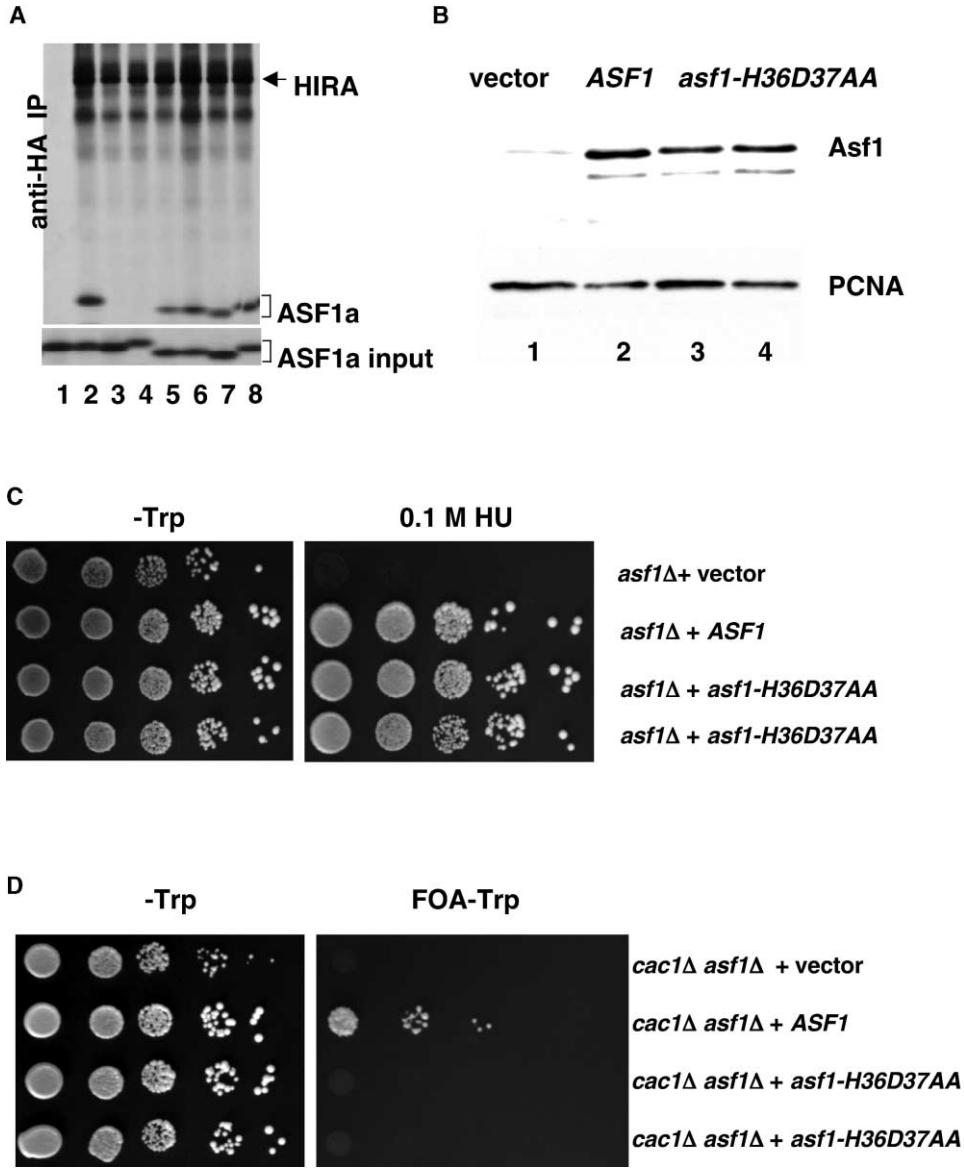

Figure 4. Surface Residues 36 and 37 Are Required for the Human Asf1a-HIRA Protein Interaction and for Asf1-Mediated Telomeric Silencing, but Not DNA Damage Resistance, in Yeast

(A) Human HA-tagged HIRA (lanes 2–8), wild-type (WT) human ASF1a (lanes 1 and 2), and a series of mutant human ASF1a proteins (lanes 3–8) were synthesized by in vitro translation in the presence of ^{35}S-methionine. Proteins were immunoprecipitated with an antibody to HA (12CA5), and bound proteins were fractionated by SDS-PAGE and visualized by fluorography. The bottom panel shows the one-fifth of the total input ASF1a. ASF1a mutants: ED36-37AA (lane 3), VGP62-64AAA (lane 4), D13A (lane 5), ESE49-51ASA (lane 6), D77A (lane 7), and ELRE121-124ALRA (lane 8).

(B) Immunoblot of total cell extracts from strains analyzed in Figure 4D. Two independent isolates of the *asf1-H36D37-AA* cells were tested in which the *H36D37-AA* mutation was made in the context of full-length Asf1. 5 μg total cell protein was probed with antibodies raised against Asf1 (top). The same blot was reprobed with antibodies that recognize PCNA as a loading control(bottom panel).

(C) Wild-type HU sensitivity of *asf1-H36D37-AA* cells. Two independent isolates of the *asf1-H36D37-AA* cells were grown and plated as described in Figure 1A.

(D) Telomeric silencing defect of *cac1 asf1-H36D37-AA* cells. Cells were grown and plated as described in Figure 1B.

pressed by insertion of *ASF1* codons 1–155 followed by two FLAG epitopes into pET28a (Novagen). Asf1N-FLAG was purified by metal affinity chromatography followed by S-200 gel filtration chromatography (Pharmacia) and Poros HQ (Roche) ion exchange chromatography. C terminally FLAG-epitope-tagged, full-length Asf1 was expressed as described [16] and purified as described above for the Asf1N-FLAG protein.

For crystallization, Asf1N was expressed in *E. coli* using a modified pET expression vector encoding an N-terminal hexa-histidine tag followed by a TEV protease cleavage site (N. Pokala and T. Handel, personal communication). The TEV cleavage site was engineered such that the N terminus after cleavage is H_2N-G-A-S-, with the S residue representing the second amino acid of natural Asf1. Asf1N was purified from cell lysates by metal affinity chromatography on Talon resin according to manufacturer's instructions (Clonetech). The histidine tag was cleaved from Asf1N by hexa-histidine-tagged TEV protease digestion at 25°C for 16 hr [48], and the TEV was subsequently removed by metal affinity chromatography. Cleaved

Asf1N was further purified by gel filtration chromatography on a Pharmacia S-200 column; peak fractions displayed an apparent molecular weight of 20 kDa, consistent with an Asf1N monomer. Purified Asf1N was concentrated to 5–10 mg/mL using a Centriprep concentrator (Millipore).

Protein Binding and Histone Deposition Assays

Histone $(H3{\cdot}H4)_2$ tetramers were purified from HeLa cell nuclei as described [49]. 75 pmol of histones $(H3{\cdot}H4)_2$ were preincubated with an equimolar amount of either Flag-Asf1 or Flag-Asf1N for 30 min at 30°C in 30 μl of histone binding buffer (30 mM Hepes-NaOH [pH 7.5], 5% glycerol, 100 mM NaCl, 0.1% Triton X-100, 0.1 mM EDTA, and 0.1 mg/mL BSA). The reactions were then incubated for 1 hr at room temperature in binding buffer with anti-Flag M2 antibody agarose beads (Sigma) in a final volume of 200 μL. Beads were washed four times with 1 ml of wash buffer (30 mM Hepes-NaOH [pH 7.5], 5% glycerol, 0.1% Triton X-100, 0.1 mM EDTA, 0.1 mg/mL BSA, and either 250 mM or 500 mM NaCl). Proteins were eluted with sample buffer and analyzed on a 17% SDS-PAGE gel stained with Coomassie blue R250.

The binding and washing buffer for the Asf1-Rad53 interaction experiments was the same used for histone binding described above except that the NaCl concentration was 100 mM. Binding was performed in a total volume of 40 μL for 30 min at 30°C prior to immunoprecipitation and washing as described above, using the 100 mM NaCl-containing buffer.

Histone deposition during in vitro DNA replication by CAF-I was assayed as described [13, 16, 30]. Complexes of purified Asf1 or Asf1N with histones H3 and H4 were formed by mixing at a 4:1 molar ratio of Asf1 to histone tetramer in binding buffer (30 mM Hepes-NaOH [pH 7.5], 100 mM NaCl, 0.1% Triton X-100, 0.1 mM EDTA, and 0.1 mg/ml BSA) and incubation at 30°C for 30 min. Replication reactions were initiated and incubated at 30°C for 20 min prior to addition of Asf1/histone complexes, and reactions were continued for 70 min.

Coimmunoprecipitation assays with in vitro-translated human Asf1a and HIRA were performed as described [50]. Protein complexes were washed five times in NETN (20 mM Tris-HCl [pH 8.0], 100 mM NaCl, 1 mM EDTA, and 0.5% NP40).

Crystallography, Data Collection, and Refinement

Prior to crystallization, concentrated Asf1N was dialyzed into 10 mM Hepes-NaOH (pH 7.5), 50 mM NaCl, and 1 mM TCEP at 4°C. Initial needle-like crystals were grown at 18°C in sitting drops by mixing 0.8 μl of a reservoir solution containing 100 mM NH_4F, 100 mM NaBr, and 20% PEG 3350 with 0.8 μl dialyzed Asf1N. Small crystals were harvested, diluted 100× in well solution, and used for macroseeding. Large, single, plate-like crystals (150 × 100 × 20) were grown in hanging drops by mixing 0.9 μl well solution (0.85–1.0 M NaBr and 17% PEG 3350), 0.9 μl Asf1N, and 0.2 μl of seed stock. Single crystals were harvested into cryoprotectant solution (10 mM HEPES-NaOH [pH 7.5], 20% PEG 3350, 25% PEG400, 1M NaBr, 50 mM NaCl, and 1 mM TCEP) and flash-frozen in liquid nitrogen.

MAD data were collected using the Advanced Light Source Beamline 8.3.1 at Lawrence Berkeley National Laboratory (Table 1). Diffraction data were processed with HKL2000 [51]. The crystals contain one molecule in the asymmetric unit (25% solvent) and belong to the space group C2 ($a = 94.36$ Å, $b = 31.7$ Å, $c = 53.6$ Å, $\alpha = \gamma = 90°$, $\beta = 124.6°$). A total of nine Br^- sites were located using SOLVE [52], and an initial model was built into the experimental electron density maps using RESOLVE [52]. Subsequent model building was carried out using O [53]. Refinement was performed using REFMAC5 and ARP [54]. The final model accounts for all residues in the Asf1N sequence, 92.7% of which fall in the most favored regions of Ramachandran space as determined by PROCHECK [55].

Acknowledgments

We thank N. Pokala and T. Handel for advice and reagents for protein expression. This work was supported by Department of Energy funds awarded to P.D.K. and administered through the Lawrence Berkeley National Laboratory, National Science Foundation Grant MCB-9982909 (P.D.K.), National Institutes of Health grant GM55712 (P.D.K.), and NIH grant GM055583 (S.J.B). J.M.B. gratefully acknowledges support from the G. Harold and Leila Y. Mathers Charitable Foundation. The work of P.D.A. is supported by NIH R01 GM62281, DAMD17-02-1-0726, and a Leukemia and Lymphoma Society Scholar award.

Received: October 10, 2003
Revised: November 4, 2003
Accepted: November 5, 2003
Published: December 16, 2003

References

1. Worcel, A., Han, S., and Wong, M.L. (1978). Assembly of newly replicated chromatin. Cell *15*, 969–977.
2. Lucchini, R., and Sogo, J.M. (1995). Replication of transcriptionally active chromatin. Nature *274*, 276–280.
3. Kaufman, P.D., and Almouzni, G. (2000). DNA replication, nucleotide excision repair, and nucleosome assembly. In Chromatin Structure and Gene Expression, Second Edition, S.C.R. Elgin and J.L. Workman, eds. (Oxford: Oxford University Press) pp. 24–48.
4. Sharp, J.A., and Kaufman, P.D. (2003). Chromatin proteins are determinants of centromere function. Curr. Top. Microbiol. Immunol. *274*, 24–52.
5. Le, S., Davis, C., Konopka, J.B., and Sternglanz, R. (1997). Two new S-phase-specific genes from *Saccharomyces cerevisiae*. Yeast *13*, 1029–1042.
6. Singer, M.S., Kahana, A., Wolf, A.J., Meisinger, L.L., Peterson, S.E., Goggin, C., Mahowald, M., and Gottschling, D.E. (1998). Identification of high-copy disruptors of telomeric silencing in *Saccharomyces cerevisiae*. Genetics *150*, 613–632.
7. Myung, K., Pennaneach, V., Kats, E.S., and Kolodner, R.D. (2003). Saccharomyces cerevisiae chromatin-assembly factors that act during DNA replication function in the maintenance of genome stability. Proc. Natl. Acad. Sci. USA *100*, 6640–6645. Published online May 15, 2003. 10.1073/pnas.1232239100.
8. Qin, S., and Parthun, M.R. (2002). Histone H3 and the histone acetyltransferase Hat1p contribute to DNA double-strand break repair. Mol. Cell. Biol. *22*, 8353–8365.
9. Formosa, T., Ruone, S., Adams, M.D., Olsen, A.E., Eriksson, P., Yu, Y., Rhoades, A., Kaufman, P.D., and Stillman, D.J. (2002). Defects in SPT16 or POB3 (yFACT) cause dependence on the Hir/Hpc pathway: accessing DNA may degrade chromatin structure. Genetics *162*, 1557–1571.
10. Umehara, T., Chimura, T., Ichikawa, N., and Horikoshi, M. (2002). Polyanionic stretch-deleted histone chaperone cia1/Asf1p is functional both in vivo and in vitro. Genes Cells *7*, 59–73.
11. Tyler, J.K., Adams, C.R., Chen, S.R., Kobayashi, R., and Kamakaka, R.T., and Kadonaga, J.T. (1999). The RCAF complex mediates chromatin assembly during DNA replication and repair. Nature *402*, 555–560.
12. Tyler, J.K., Collins, K.A., Prasad-Sinha, J., Amiott, E., Bulger, M., Harte, P.J., Kobayashi, R., and Kadonaga, J.T. (2001). Interaction between the Drosophila CAF-1 and ASF1 chromatin assembly factors. Mol. Cell. Biol. *21*, 6574–6584.
13. Krawitz, D.C., Kama, T., and Kaufman, P.D. (2002). Chromatin assembly factor-I mutants defective for PCNA binding require Asf1/Hir proteins for silencing. Mol. Cell. Biol. *22*, 614–625.
14. Mello, J.A., Sillje, H.H., Roche, D.M., Kirschner, D.B., Nigg, E.A., and Almouzni, G. (2002). Human Asf1 and CAF-1 interact and synergize in a repair-coupled nucleosome assembly pathway. EMBO Rep. *3*, 329–334.
15. Sutton, A., Bucaria, J., Osley, M.A., and Sternglanz, R. (2001). Yeast ASF1 protein is required for cell-cycle regulation of histone gene transcription. Genetics *158*, 587–596.
16. Sharp, J.A., Fouts, E.T., Krawitz, D.C., and Kaufman, P.D. (2001). Yeast histone deposition protein Asf1p requires Hir proteins and PCNA for heterochromatic silencing. Curr. Biol. *11*, 463–473.
17. Kaufman, P.D., Cohen, J.L., and Osley, M.A. (1998). Hir proteins are required for position-dependent gene silencing in *Saccharo-*

myces cerevisiae in the absence of chromatin assembly factor I. Mol. Cell. Biol. *18*, 4793–4806.

18. Hall, C., Nelson, D.M., Ye, X., Baker, K., DeCaprio, J.A., Seeholzer, S., Lipinski, M., and Adams, P.D. (2001). HIRA, the human homologue of yeast Hir1p and Hir2p, is a novel cyclin-cdk2 substrate whose expression blocks S-phase progression. Mol. Cell. Biol. *21*, 1854–1865.
19. Nelson, D.M., Ye, X., Hall, C., Santos, H., Ma, T., Kao, G.D., Yen, T.J., Harper, J.W., and Adams, P.D. (2002). Coupling of DNA synthesis and histone synthesis in S phase independent of cyclin/cdk2 activity. Mol. Cell. Biol. *22*, 7459–7472.
20. Ray-Gallet, D., Quivy, J.P., Scamps, C., Martini, E.M., Lipinski, M., and Almouzni, G. (2002). HIRA is critical for a nucleosome assembly pathway independent of DNA synthesis. Mol. Cell *9*, 1091–1100.
21. Emili, A., Schieltz, D.M., Yates, J.R., and Hartwell, L. (2001). Dynamic interaction of DNA damage checkpoint protein Rad53 with chromatin assembly factor Asf1. Mol. Cell *7*, 13–20.
22. Hu, F., Alcasabas, A.A., and Elledge, S.J. (2001). Asf1 links Rad53 to control of chromatin assembly. Genes Dev. *15*, 1061–1066.
23. Osada, S., Sutton, A., Muster, N., Brown, C.E., Yates, J.R., 3rd, Sternglanz, R., and Workman, J.L. (2001). The yeast SAS (something about silencing) protein complex contains a MYST-type putative acetyltransferase and functions with chromatin assembly factor ASF1. Genes Dev. *15*, 3155–3168.
24. Meijsing, S.H., and Ehrenhofer-Murray, A.E. (2001). The silencing complex SAS-I links histone acetylation to the assembly of repressed chromatin by CAF-I and Asf1 in Saccharomyces cerevisiae. Genes Dev. *15*, 3169–3182.
25. Moshkin, Y.M., Armstrong, J.A., Maeda, R.K., Tamkun, J.W., Verrijzer, P., Kennison, J.A., and Karch, F. (2002). Histone chaperone ASF1 cooperates with the Brahma chromatin-remodelling machinery. Genes Dev. *16*, 2621–2626.
26. Chimura, T., Kuzuhara, T., and Horikoshi, M. (2002). Identification and characterization of CIA/ASF1 as an interactor of bromodomains associated with TFIID. Proc. Natl. Acad. Sci. USA *99*, 9334–9339.
27. Sanders, S.L., Jennings, J., Canutescu, A., Link, A.J., and Weil, P.A. (2002). Proteomics of the eukaryotic transcription machinery: identification of proteins associated with components of yeast TFIID by multidimensional mass spectrometry. Mol. Cell. Biol. *22*, 4723–4738.
28. Sutton, A., Shia, W.J., Band, D., Kaufman, P.D., Osada, S., Workman, J.L., and Sternglanz, R. (2003). Sas4 and Sas5 are required for the histone acetyltransferase activity of Sas2 in the SAS complex. J. Biol. Chem. *278*, 16887–16892.
29. Gottschling, D.E., Aparicio, O.M., Billington, B.L., and Zakian, V.A. (1990). Position effect at *S. cerevisiae* telomeres: reversible repression of PolII transcription. Cell *63*, 751–762.
30. Kaufman, P.D., Kobayashi, R., and Stillman, B. (1997). Ultraviolet radiation sensitivity and reduction of telomeric silencing in *Saccharomyces cerevisiae* cell lacking chromatin assembly factor-I. Genes Dev. *11*, 345–357.
31. Munakata, T., Adachi, N., Yokoyama, N., Kuzuhara, T., and Horikoshi, M. (2000). A human homologue of yeast anti-silencing factor has histone chaperone activity. Genes Cells *5*, 221–233.
32. Schwartz, M.F., Lee, S., Duong, J.K., Eminaga, S., and Stern, D.F. (2003). FHA domain-mediated DNA checkpoint regulation of Rad53. Cell Cycle *2*, 384–396.
33. Bork, P., Holm, L., and Sander, C. (1994). The immunoglobulin fold. Structural classification, sequence patterns and common core. J. Mol. Biol. *242*, 309–320.
34. Murzin, A.G., Brenner, S.E., Hubbard, T., and Chothia, C. (1995). SCOP: a structural classification of proteins database for the investigation of sequences and structures. J. Mol. Biol. *247*, 536–540.
35. Fattorusso, R., Pellecchia, M., Viti, F., Neri, P., Neri, D., and Wuthrich, K. (1999). NMR structure of the human oncofoetal fibronectin ED-B domain, a specific marker for angiogenesis. Struct. Fold. Des. *7*, 381–390.
36. Keep, N.H., Barnes, M., Barsukov, I., Badii, R., Lian, L.Y., Segal, A.W., Moody, P.C., and Roberts, G.C. (1997). A modulator of rho family G proteins, rhoGDI, binds these G proteins via an immunoglobulin-like domain and a flexible N-terminal arm. Structure *5*, 623–633.
37. Akey, C.W., and Luger, K. (2003). Histone chaperones and nucleosome assembly. Curr. Opin. Struct. Biol. *13*, 6–14.
38. Ridgway, P., and Almouzni, G. (2000). CAF-1 and the inheritance of chromatin states: at the crossroads of DNA replication and repair. J. Cell Sci. *113*, 2647–2658.
39. Verreault, A. (2000). De novo nucleosome assembly: new pieces in an old puzzle. Genes Dev. *14*, 1430–1438.
40. Neer, E.J., Schmidt, C.J., Nambudripad, R., and Smith, T.F. (1994). The ancient regulatory-protein family of WD-repeat proteins. Nature *371*, 297–300.
41. Wall, M.A., Coleman, D.E., Lee, E., Iniguez-Lluhi, J.A., Posner, B.A., Gilman, A.G., and Sprang, S.R. (1995). The structure of the G protein heterotrimer Gi alpha 1 beta 1 gamma 2. Cell *83*, 1047–1058.
42. Dutta, S., Akey, I.V., Dingwall, C., Hartman, K.L., Laue, T., Nolte, R.T., Head, J.F., and Akey, C.W. (2001). The crystal structure of nucleoplasmin-core: implications for histone binding and nucleosome assembly. Mol. Cell *8*, 841–853.
43. Namboodiri, V.M., Dutta, S., Akey, I.V., Head, J.F., and Akey, C.W. (2003). The crystal structure of *Drosophila* NLP-core provides insight into pentamer formation and histone binding. Structure (Camb) *11*, 175–186.
44. Dilworth, S.M., Black, S.J., and Laskey, R.A. (1987). Two complexes that contain histones are required for nucleosome assembly in vitro: role of nucleoplasmin and N1 in *Xenopus* egg extracts. Cell *51*, 1009–1018.
45. Ito, T., Tyler, J.K., Bulger, M., Kobayashi, R., and Kadonaga, J.T. (1996). ATP-facilitated chromatin assembly with a nucleoplasmin-like protein from Drosophila melanogaster. J. Biol. Chem. *271*, 25041–25048.
46. McBryant, S.J., Abernathy, S.M., Laybourn, P.J., Nyborg, J.K., and Luger, K. (2003). Preferential binding of the histone (H3–H4)2 tetramer by NAP1 is mediated by the amino terminal histone tails. J. Biol. Chem. *278*, 44574–44583. Published online August 19, 2003. 10.1074/jbc.M305636200.
47. Sikorski, R.S., and Hieter, P. (1989). A system of shuttle vectors and yeast host strains designed for efficient manipulation of DNA in *Saccharomyces cerevisiae*. Genetics *122*, 19–27.
48. Kapust, R.B., and Waugh, D.S. (1999). Escherichia coli maltose-binding protein is uncommonly effective at promoting the solubility of polypeptides to which it is fused. Protein Sci. *8*, 1668–1674.
49. Simon, R.H., and Felsenfeld, G. (1979). A new procedure for purifying histone pairs H2A + H2B and H3 + H4 from chromatin using hydroxylapatite. Nucleic Acids Res. *6*, 689–696.
50. Adams, P.D., Sellers, W.R., Sharma, S.K., Wu, A.D., Nalin, C.M., and Kaelin, W.G., Jr. (1996). Identification of a cyclin-cdk2 recognition motif present in substrates and p21-like cyclin-dependent kinase inhibitors. Mol. Cell. Biol. *16*, 6623–6633.
51. Otwinowski, Z., and Minor, W. (1997). Processing of X-Ray Diffraction Data Collected in Oscillation Mode, Methods in Enzymology, Volume 276: Macromolecular Crystallography, Part A, pp. 472–494, C.W. Carter, Jr., and R.M. Sweet, eds., Academic Press.
52. Terwilliger, T., and Berendzen, J. (1999). Automated structure solution for MIR and MAD. Acta Crystallogr. *D55*, 849–861.
53. Jones, T.A., Zou, J.Y., Cowan, S.W., and Kjeldgaard, M. (1991). Improved methods for building protein models in electron density maps and the location of errors in these models. Acta Crystallogr. A *47*, 110–119.
54. Lamzin, V.S., and Wilson, K.S. Automated Refinement for Protein Crystallography. Methods in Enzymology, Volume 277, pp. 269–305, C.W. Carter, Jr., and R.M. Sweet, eds., Academic Press.
55. Laskowski, R., MacArthur, M., Moss, D., and Thornton, J. (1993). PROCHECK: a program to check the stereochemical quality of protein structures. J. Appl. Crystallogr. *26*, 283–291.
56. Thompson, J.D., Gibson, T.J., Plewniak, F., Jeanmougin, F., and Higgins, D.G. (1997). The CLUSTAL_X windows interface: flexible strategies for multiple sequence alignment aided by quality analysis tools. Nucleic Acids Res. *25*, 4876–4882.

57. DeLano, W.L. (2002). The PyMOL Molecular Graphics System (San Carlos, CA: DeLano Scientific).
58. Barton, G.J. (1993). ALSCRIPT: a tool to format multiple sequence alignments. Protein Eng. *6*, 37–40.
59. Nicholls, A., Sharp, K.A., and Honig, B. (1991). Protein folding and association: insights from the interfacial and thermodynamic properties of hydrocarbons. Proteins Struct. Funct. Genet. *11*, 281–296.
60. Glaser, F., Pupko, T., Paz, I., Bell, R.E., Bechor-Shental, D., Martz, E., and Ben-Tal, N. (2003). ConSurf: identification of functional regions in proteins by surface-mapping of phylogenetic information. Bioinformatics *19*, 163–164.

Accession Numbers

Coordinates for Asf1N have been deposited in the Protein Data Bank under ID code 1ROC.